DEVELOPMENT OF A NONDESTRUCTIVE BEAM PROFILE MONITOR USING A SHEETED NITROGEN-MOLECULAR BEAM *

Y. Hashimoto#, S. Muto, T. Toyama, T. Morimoto, KEK, Tsukuba, Japan
T. Fujisawa, T. Murakami, K. Noda, NIRS, Chiba, Japan
D. Ohsawa, Kyoto Univ., Kyoto, Japan

Abstract

A non-destructive beam profile monitor using a sheeted nitrogen-molecular beam as a target has been developed for intense ion beams. The pressure of the sheeted molecular beam was 5 x 10^{-4} Pa at the beam collision point. A light emitted from excited nitrogen by an ion beam collision is measured by a high sensitive camera with a radiation resistant image intensifier. In tests, beam profiles of 6 MeV/n full-stripped oxygen beams whose average current was 540 μA were successfully measured.

INTRODUCTION

An advantage of using light in beam profile measurement is free from electro-magnetic field induced by charged beam. By using a thin molecular target, emitted point of the light becomes clear. Also by using an imaging tube, two-dimensional beam profile can be taken. On the other hands, high beam intensity or higher beam repetition or both is required to obtain a meaningful beam profile in GeV-class energy of accelerator, because the light is not so intense.

For a general method to measure beam profile non-destructively, the residual gas is used[1,2]. Ions or electrons produced by beam collisions are led to a micro channel plate (MCP) by guiding electrostatic field or electrostatic and magnetostatic fields with keep the spatial distribution of ions and electrons, and they are multiplied by MCP. At the MCP anode, multiplied electrons are read out with divided strips generally. In case of an intense beam, stronger guiding fields are required to overcome beam induced fields. In this method, beam profile can be obtained as a spatial projection.

The other non-destructive methods are applied in TeV-class energy of accelerators such as the Tevatron and the LHC. They are employing radiated light[3] from bending magnet or wiggler[4], respectively.

In the present method, to increase detected yields of light, the pressure of nitrogen-molecular beam and detector sensitivity should be both higher. In a case of intense beam, radiation proof of MGy-class is required to their equipments.

EMITTED LIGHT FROM NITROGEN

For light detection for the nitrogen molecular target, the light of the wave lengths of 391.4 and 427.8 nm [5, 6] are used. These lights are emitted in de-exciting process of N^+ ion produced by beam collision. The yields of these lights are primary and secondary peaks of nitrogen molecular spectrum in visible light region. The time constant of light decay is both 58 ns, which has an advantage to detect a fast phenomenon such as one bunch shape.

Cross sections of a proton on the above mentioned reaction are shown in reference of [5]. Total cross sections of the visible wave lengths light are 1 x 10^{-18} and 2.6 x 10^{-20} cm^2, on proton beam energies of 6 MeV and 3GeV, respectively. These values are used in later discussions, the 6 MeV's case is for a beam test, the 3GeV's case is for yield estimation of GeV-class intense beams.

MOLECULAR BEAM GENERATOR

Layout of the sheeted molecular beam generator and its representative parameters are shown in Fig. 1 and Table 1, respectively. A nitrogen molecular beam is generated by a nozzle and a skimmer with high pressure gas source which operated by pulse valve.

Table 1: Molecular Beam's and Generator's Specifications.

ITEM	Parameter
Gas Species	N_2
Pressure of Molecular Beam	5 x 10^{-4} Pa
Pulse duration	100-1000 μs
Source Pressure	0.8 MPa
Nozzle Size	2.4 mm^{ϕ}
1st/2nd Skimmer Size	3.5^H x 3.5^V/2.0^H x 20^V mm^2
Target Cross Sectional Size	53^W x 5^t

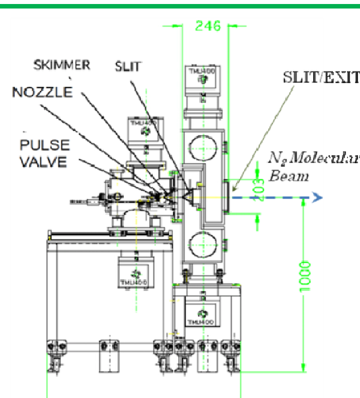

Figure 1: Layout of the sheeted molecular beam generator.

The nitrogen molecular beam is cooled down to temperature of about 15K by each other's collision around the nozzle exit. The beam state is supersonic of Mach 10[7]. The beam velocity is about 800 mm/ms, so it takes 0.5 ms from the nozzle to the exit of the generator. The thickness of the molecular target can be varied by a final slit positioned at the exit part of the generator. Specifications of the molecular beam are summarized in Table 1. The data was measured by an ionization gauge

*Work supported by JSPS KAKENHI 18340078.
#yoshinori.hashimoto@kek.jp

covered with compression chamber and connected to a fast charge amplifier of Keithley 428. A spatial distribution of a sheeted molecular beam in direction of width is shown in Fig.2.

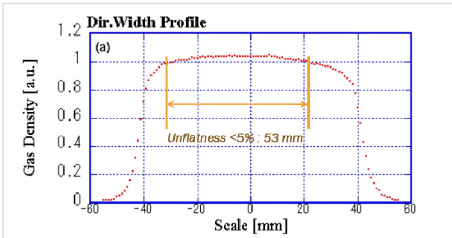

Figure 2: A spatial distribution of the sheeted molecular beam at beam collision point. A width of un-flatness less than 5% is 53 mm.

DETECTOR

An overview of the detection system for beam profile measurement is shown in Fig. 3.

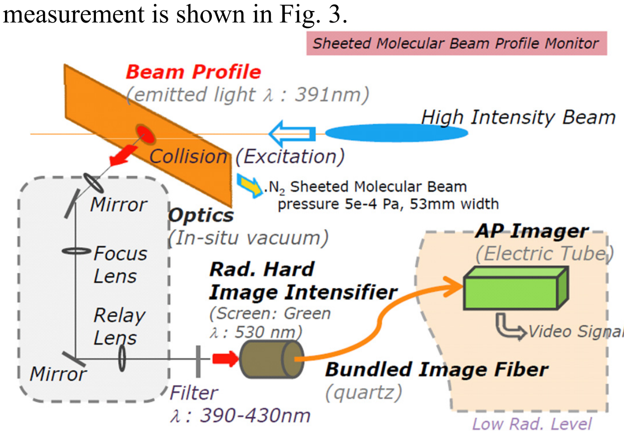

Figure 3: Overview of the detection system.

Optical System

The optical system mentioned below is now under construction. The main concept of the design is how to reduce a transmission loss of the light from the target to the image intensifier. The first lens should be positioned as close as possible to the target, and the aperture should be large. An optical system under reviewing consists of a focusing and a relaying section.

Prospective materials are quartz for lenses and Ti + MgF_2 [8] for mirror coating from viewpoint of radiation proof. For reducing a spherical aberration, it is also under investigation for using an aspheric surface lens for the first lens. So the wave lengths of detecting light is 390-430 nm, chromatic aberration need not be considered.

The optical system is situated in a vacuum chamber to avoid influences of the light from atmospheric nitrogen by collisions with secondary particles.

Radiation Resistant Image Intensifier Tube (IIT)

Because a usual image intensifier tube (IIT) is not always resistant for radiation damage, irradiation tests for some parts of the system were carried out with γ-ray. After 1MGy irradiation, fiber optic plate(FOP) and borosilicate glass which are used in the glass part, PTFE in the high voltage feeder, an engineering plastic of polyacetal in housing, and a resin for potting in the case were damaged [9]. Depending on the results, defective materials are modified. Changed materials are as below, synthetic silica for glass, PEEK for cable insulation, a resin consists of halogen freed Epoxy with Polyimide and radical-trap resin, which was made by the CITIZEN WATCH, Co. Ltd, for potting material. Finally this improved radiation resistant IIT was manufactured for commercial products C4274RTH with cooperated efforts by the HAMAMATSU PHOTONICS, K.K.. The IIT head has a two stages MCP built-in. Its controller can be positioned 100m apart, and is connected to IIT with a PEEK cable. Its gate-pulse width is variable between 500 ns and DC. The phosphor light is transmitted to the next detector of AP Imager (API) with bundled image fibers. The background due to the Cherenkov light produced in the bundle image fibers by scattered charged particle is foreseen. Thus, by changing the color of the phosphor light, it is expected that the background can be discriminated easily from the true signal. The phosphor screen was changed into P46 (light green, wave length: 530 nm) from usual P47 (blue, wave length: 430 nm). Although the light decay time of P46 phosphor is 300 ns at 1/10, which is three times longer than P47's, it is sufficiently short for detecting bunches in case of repetition rate of 2 MHz or less.

AP Imager (API)

API is one of high gain electric tubes for imaging. Its multiplying is done by avalanche effect for photo electron in a thin amorphous selenium foil. Its advantages are higher signal-to-noise ratio(S/N) than the other imaging tubes, and a wide dynamic range of four orders of magnitude. The gain of multiplying is about 200. API is set up remotely and under circumferences of relatively low background.

BEAM TEST

A beam test was carried out using O^{8+} beam whose energy is 6 MeV/n at intermediate energy experiment hall in the HIMAC, NIRS. The set up is shown in Fig. 4. Beam and detector parameters are listed in Table 2.

Table 2: Parameters of beam and detector on the test .

ITEM	Parameter
Optical Lens	f25 mm/F1.8
Distance of Lens to Beam	175 mm
IIT Luminous Gain (Max.5e4)	3 x10^2 (lm/m^2)/lx
API photo electron Gain (Max.200)	200
Beam Species	O^{8+}
Averaged Beam Current (Beam Intensity)	540 μA (2 x 10^{11} ppp)
Beam Pulse Duration	700 μs
Averaging	30

In the measurement, a wide angle macro lens was attached to the IIT, and the distance between the collision point and the lens front was 175 mm. Also, the bundled image fiber was not employed. A beam profile was measured successfully, as shown in Fig. 5. The reason why the vertical beam size was larger, is that target was inclined 45 degree. Thus the vertical beam size was biased with the target effective thickness of 7 mm. So the horizontal and vertical beam sizes in FWHM were 2 mm^H and 1.5 mm^V, respectively. They were consistent with another measurement by screen monitor in the same point.

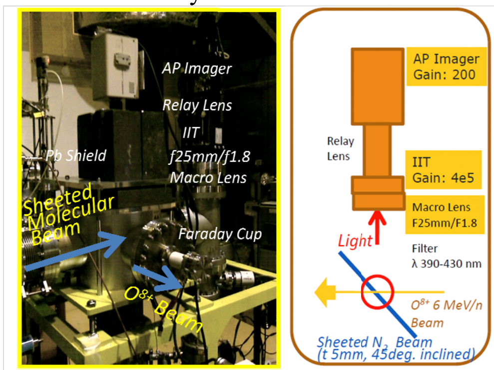

Figure 4: Setup for HIMAC beam test. A photo and cross-sectional overview of collision point and instruments.

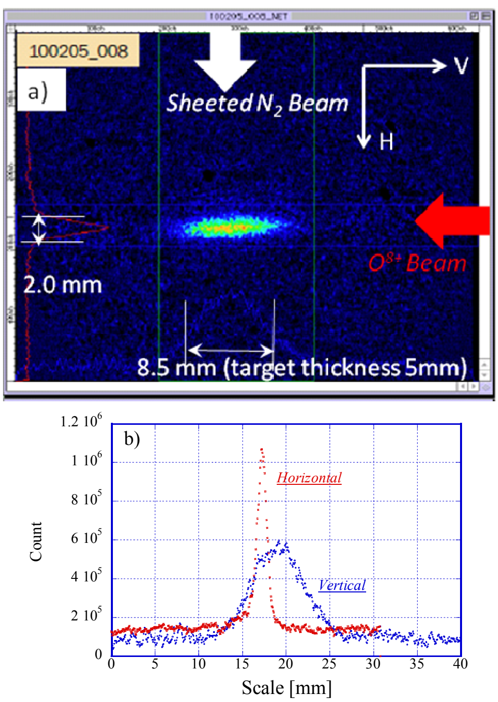

Figure 5: A beam profile of O^{8+} beam at energy of 6MeV/n. In a picture of a), a sheeted N_2 molecular beam was across the O^{8+} beam from upside to downside with inclined angle of 45 degree. b) shows projected profiles.

The cross-section value in beam collision of O^{8+} is treated effectively by multiplying the 6 MeV proton's data described before by square of the valence of 8, and the value is 6.4×10^{-17} cm^2. An estimated number of the yielded photon at the entrance of IIT was 7×10^4 in this measurement. In this case, the IIT gain was 3×10^2 lm/m^2/lx. This value was very row against its maximum of 5×10^4 lm/m^2/lx. In case of higher IIT gain than this measurement, spatial light noises were increased and then the S/N became poorer. It would appear that secondary particle produced at the faraday cup positioned 30 cm downstream came into the IIT.

OFFLINE TEST

As the beam intensity is higher, the light yield per unit time is larger. Also detection with better S/N is expected. Offline tests were done for an investigation for intense proton beam of GeV-class. Detector setup was the same as the beam test mentioned above, in addition LED was employed for a light source, and neutral density filters were used for varying light quantity.

An offline test for intense proton beam whose assuming intensity and energy are 4 x 10^{13} ppb and 3 GeV respectively was carried out. Result is shown in Fig. 6 (b). In the figure, (a) corresponds to the beam test demonstrates for comparison. In the case of (a), the IIT gain was set for 3×10^2 lm/m^2/lx, the gate time was set for 700µs, they were the same as the beam test condition. In the case of (b), the IIT gain was set for 3×10^4 lm/m^2/lx, the gate time was set for 500ns which corresponds to almost 5 bunches. Because it is estimated that a light quantity of the beam test corresponds to a light quantity yielded by 5 bunches in above intense beam case.

A detected light in case of (b) was 85 times larger than case of (a). Also in the case of (b), S/N was adequately higher than the case of (a).

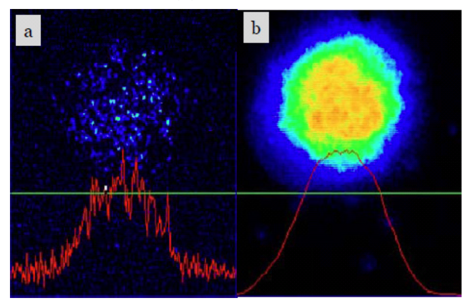

Figure 6: An offline test with LED light source. a) corresponds to HIMAC O^{8+} beam test, b) corresponds to 3GeV beam of which intensity is 4 x 10^{13} ppb. Both (a) and (b) are 30 averaged. Red lines mean projections to the horizontal axis.

SUMMARY

With sheeted nitrogen molecular target, a profile of O^{8+} beam whose energy was 6 MeV/n was successfully measured. High-sensitive detector which consisted of a radiation resistant image intensifier and an AP imager were investigated on beam profile detection. In an offline test with LED source, assuming 3GeV proton whose intensity is 4×10^{13} ppb x 5 bunches, it estimates yielded light is enough for beam profile measurement, and S/N is sufficiently higher.

The authors express their appreciation to accelerator's crew of the HIMAC, NIRS for their helpful support.

REFERENCES

[1] K. Satou, *et al.*, Proc. of Hadron Beam 2008, p.472-474.
[2] H. Weisberg, *et al.*, IEEE Trans. Nucl. Sci., Vol. NS-30(1983) 2179-2181.
[3] H. W. K. Cheung, Proc. of PAC, 2003, p.2488-2490.
[4] A. S. Fisher, *et al.*,Proc. of DIPAC2009, p.164-166.
[5] M. A. Plum, *et al.*, NIM A, 492(2002)74-79.
[6] G. Burtin, *et al.*, Proc. of EPAC2000, p.256-258.
[7] Y. Hashimoto, *et al.*, NIM A 527 (2004) 289-300.
[8] Y. Takeda, *et al.*, NIM A 590(2008)213-220.
[9] J. Kusano, edited, JAEA-Review, 2008-022, p.87-88.